Supplementary Materials for

A Trojan horse route to emergent active and stable platinum nanoparticles

Maadhav Kothari[1,†], Yukwon Jeon[1,†], David N. Miller[1], Andrea Eva Pascui[2], John Kilmartin[2], David Wails[2], Silvia Ramos[3], Alan V. Chadwick[3] and John T.S. Irvine[1*]

*Correspondence to: jtsi@st-andrews.ac.uk (Prof. John T.S. Irvine).
†These authors contributed equally to this work.

This PDF file includes:

Materials and Methods
Figs. S1 to S15
Tables S1 to S4

Glossary Schematic

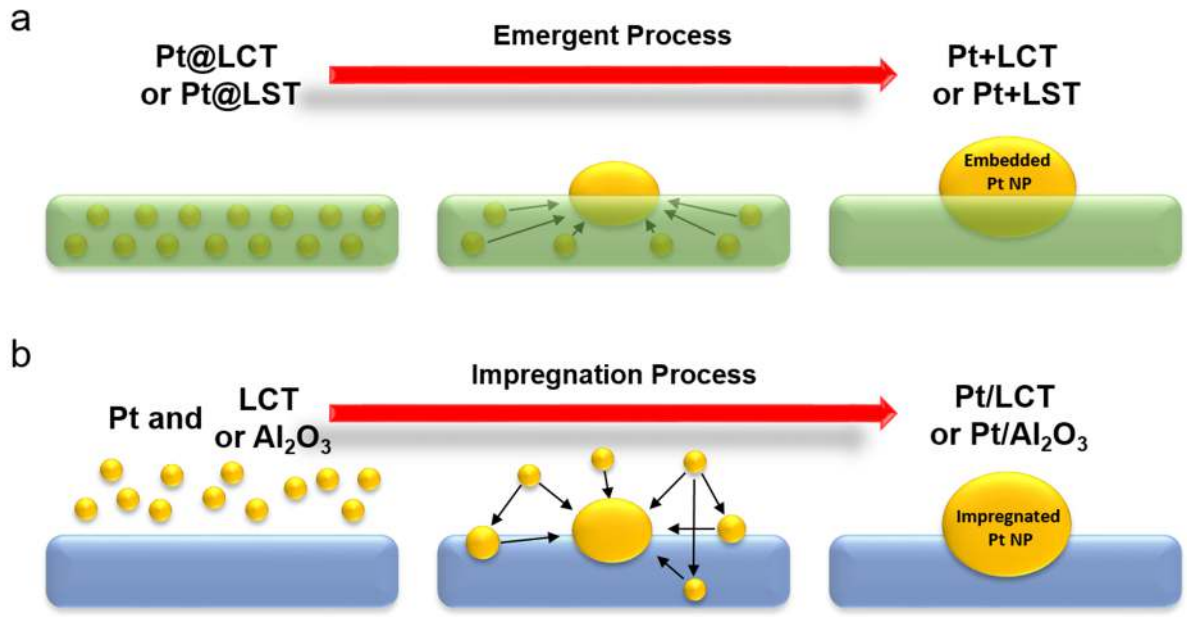

Schematic Figure of the comparison on Pt nanoparticle formation processes. (a) Emergent process and (b) Impregnation process.

Materials and Methods

Precursors.

High purity oxide and carbonate precursors, such as La_2O_3 (Pi-Kem, >99.99%) and TiO_2 (Alfa Aesar, >99.6%), $BaCO_3$ (Alfa Aesar, >99%), $CaCO_3$ (Fisher Chemical, >99%) and $SrCO_3$ (Aldrich, >99.9%), are dried at 300 ºC (La_2O_3 at 800 ºC) in order to remove water bound molecules from the precursors for a correct stoichiometric nature of the perovskites. PtO_2 (Alfa Aesar, anhydrous) and Pt nitrate solution (Johnson Matthey, 16.17 wt% Pt) are used as Pt precursors, and $\gamma-Al_2O_3$ (Sasol, Particle size $\leq$ 5 mm, S_{BET} 138−158 m^2/g) is purchased.

Trojan horse co-precursor $Ba_3Pt_2O_7$.

$BaCO_3$ and PtO_2 are weighed and mixed together in the correct stoichiometric amount in a Pt crucible, and then fired in ~~a static~~ air in a furnace with a ramp rate of 5 ºC/min to 1000°C for 12 hrs.

Pt doped Perovskite synthesis.

A-site deficient perovskites of $La_{0.4}Ca_{0.3925}Ba_{0.0075}Pt_{0.005}Ti_{0.995}O_3$ (**Pt@LCT**) and $La_{0.4}Sr_{0.3925}Ba_{0.0075}Pt_{0.005}Ti_{0.995}O_3$ (**Pt@LST**) are designed by containing 0.5 wt% of Pt. Non-doped perovskites of $La_{0.4}Ca_{0.4}TiO_3$, $La_{0.4}Sr_{0.4}TiO_3$, $La_{0.4}Ca_{0.3925}Ba_{0.0075}TiO_3$, and $La_{0.4}Sr_{0.3925}Ba_{0.0075}TiO_3$ are prepared as references. Carefully calculated precursor quantities are quantitatively transferred to a glass beaker, then acetone is added to the beaker with a co-polymer dispersant (Hypermer KD-1, a polyester copolymer surfactant). The mixture is pulse sonicated using an ultrasonic probe (Heilscher UP200S) in order to homogenise and reduce the particle size of the precursors. Following dispersion, acetone is evaporated from the homogeneous solution and the compositional mixture is then calcined in a muffle furnace at 1000 ºC for 12 hrs to partially form the perovskite phase for seeding crystallisation. Following calcination, the sample is ball milled with acetone at 300 rpm for 2 hrs in a planetary ball mill, using 1 mm zirconia balls. Then, the sample is dried in an evaporator dish at room temperature.

O_2-rich sintering process.

Pellets are prepared by pressing the sample powders and then firing them under O_2-rich sintering conditions to produce pure perovskite phase at the relatively low temperatures. Pellets are fired for 12 hrs at 1200 ºC with a ramp rate of 5 ºC/min in an O_2-rich gas atmosphere of 100% O_2 and 100 $ml \cdot min^{-1}$.

In-situ emergence process.

To emerge the Pt NPs onto the perovskite surface, samples are chemically reduced in a controlled atmosphere furnace at 700 ºC for 12 hrs with heating and cooling rates of 5 $°C \cdot min^{-1}$ under continuous flow of 5% H_2/Ar (20 $ml \cdot min^{-1}$). The emerged Pt perovskites are denoted as **Pt+LCT** and **Pt+LST**.

Reference samples.

For a comparison, Pt impregnated LCT (**Pt/LCT**) and **Pt/$\gamma-Al_2O_3$** catalysts are synthesized by the incipient wetness method. Constant Pt concentration of 0.5 wt% was impregnated to the supports by a Pt nitrate solution, then dried at 110 °C for 24 hrs and calcined at 550 °C for 3 hrs in air. The **Pt/LCT** and **Pt/$\gamma-Al_2O_3$** samples are reduced in 5% H_2/Ar flow for 12 hrs at 700 ºC and 500 ºC, respectively.

X-ray Powder Diffraction (XRD).

XRD measurements are carried out at room temperature with an x-ray angle from 10-90^{o} by using a PAN analytical Empyrean diffractometer with CuKα1 radiation (1.54056Å) and Bragg-Brentanon geometry operated in reflection mode. STOE Win XPOW software is used to analyze the diffraction pattern and interoperate the crystal structure and cell parameter. GSAS open source refinement software is applied for carrying out Rietveld refinement of the results to find out the original perovskite phase and structural changes. The structural information is then used to construct the crystal structure by using Crystal Maker for Windows software.

X-ray absorption spectra (XAS).

The X-ray absorption near edge structure (XANES) and extended X-ray absorption fine structure (EXAFS) of the Pt L_{III}-edge for selected samples are collected at ambient temperature, on the B18 station at Diamond Light Source national synchrotron facility, UK. Measurements are carried out using a Si(111) monochromator at Pt L_{III}-edge with a Pt monometallic foil (10 μm) used as an energy calibrant. Samples are pressed into 13 mm pellets, and high Pt loaded samples are diluted using appropriate amount of cellulose binder. Pt foil and PtO_2 are used as references for Pt^0 and Pt^{4+}, respectively. XAS data analysis was carried out with the software of Athena and Artemis (*2*).

EXAFS fitting

The EXAFS functions were Fourier transformed in the *k* range of 3–13.86 $Å^{-1}$ and multiplied by a Hanning window. The basic structural model was a (fcc) Pt metal core from the ICSD code of 243678. The structure refinement was carried out using ARTEMIS software (IFFEFIT) (*2*). Moreover, the theoretical backscattering amplitudes and phases were calculated by FEFF 6.0. Then, the theoretical data corresponding to the first Pt–Pt shell were adjusted to the experimental spectra by a least square method in R-space from 1.8 to 3.12 Å. The amplitude reduction factors (S_0^2) were calculated using Pt foil model, based on the coordination number (*N*) of 12. The other fitting parameters were σ^2 (Debye-Waller factor: mean square deviation of interatomic distances), *R* (Average interatomic distance, R_{eff}: 2.77410 for Pt-Pt), ΔE0 (Energy shifts: inner potential correction between the samples and the FEFF calculation). The R-factor represents the absolute misfit allowed for the data range that were fittined between theory and experiment. The number of the independent points according to the Nyquist criterion was 8.86 and the number of the fitting parameters was 4.

Scanning electron microscope (SEM) and particle tracking.

FEI Scios electron microscope equipped with secondary and backscattered electron detector is used to acquire high-resolution images for investigating surface morphology and phase homogeneity, especially the Pt NPs distributed on the sample surfaces. To track the Pt NPs, the number and size on the surfaces are calculated for particle size distribution histograms from the adequately magnified images using Image-Pro Plus software. The selected SEM images are converted to binary images where particles are distinguished by the pixel contrast. Particle sizes are calculated by a calibration of the SEM image scale between pixel and nm, where the particles are assumed to be a hemispheric.

High-resolution transmission electron microscopy (HR-TEM).

To analyse more in detail about the morphological and elementary study on the Pt on the sample, HR-TEM imaging is carried out by the FEI Titan Themis instrument, using a 25 keV He^+ beam with 0.2 pA beam current. The elementary study through the energy dispersive X-ray (EDX) are also performed by spot and mapping analysis to distinguish the Pt NPs on the sample surface compare to the desired perovskite compositions (La, Ca, Ba, Pt, Ti, and O).

Thermogravimetric analysis (TGA).
TGA measurements are carried out on a NETZSCH STA 449 C instrument using Proteus thermal analysis software. The initial weight of the sample is about 20 mg. The buoyancy effect is corrected using empty crucible blank runs under corresponding chemical reduction gas atmosphere of flowing 5% H_2/Ar (30 ml/min). First, the sample is heated up to 1000 °C with a heating rate of 5 °C min^{-1}. Second, the sample is heated up to 700 °C with a heating rate of 5 °C min^{-1} and kept for 15 hrs.

N_2 isothermal analysis. Specific surface area (S_{BET}), average pore volume and pore size of the prepared samples are determined by the distribution graph of N_2 adsorption-desorption at 77 K using Micromeritics TRISTAR II 3020. Samples are outgassed at 150 °C under vacuum for 12 hr using a Quantachrome Flovac degasser (Micromeritics VacPrep 061). N_2 isothermal data set were collected at -195 °C. S_{BET} is calculated by the Brunauer-Emmett-Teller multiple point method at partial pressure range from 0.05 to 0.3. Total pore volume is determined at p/p_0=0.99.

X-ray photoelectron spectroscopy (XPS).
The O 1s XPS spectra are collected by thermo Scientific K-Alpha instrument equipped with monochromatic Al X-ray source (Al Kα, 1486.6 eV), using a hemispherical energy analyzer. The samples are fixed on carbon tape and all binding energies are calibrated using C 1s (284.8 eV). The results are analysed and fitted using Fityk software by a linear type background subtraction and appropriate curve shape fitting.

Initial lab-scale tests on catalytic CO oxidation and stability aging.
The catalytic performances of as-synthesized samples for CO oxidation are evaluated in a laboratory scale fixed–bed quartz reactor (internal d8 mm) under atmospheric pressure. The temperature is controlled by the K-type thermocouple at the centre of the reaction zone and gas flows are controlled by the electronic mass-flow controllers (MFC, ALICAT scientific). Approximately 200 mg of samples are grounded and sieved to 40-60 mesh to load into the reactor by quartz wool at each side. The samples are pre-treated in-situ with 5% H_2/Ar at 300 ºC for 1 hr, and then purged with N_2 for 30 min to remove the residual H_2. After cooling to 70 ºC, a feed mixture gas of 20,000 ppm CO, 10.0 vol.% O_2 from air (21% O_2 and 79% N_2) at N_2 balance is introduced with a total gas flow rate of 200 ml·min^{-1} (GHSV=60,000/hr). The light-off experiments are measured at the range of 70-300 ºC with a ramp rate of 3 ºC·min^{-1}, sampling performed every 10 ºC. At a fixed CO concentration and GHSV, the oxygen partial pressures for CO oxidation reaction are varied by 1, 5 and 10 vol.% O_2 from air (21% O_2 and 79% N_2). The composition of the effluent gas products is measured by on-line TCD gas chromatography (GC-2014, SHIMADZU) equipped with a molecular sieve 5A (60-80 mesh) column. The CO conversion is calculated by the change of the CO concentrations.

Static aging and redox aging tests (Table S4) were performed to evaluate likely stability of the catalysts in real-life conditions. These accelerated aging tests are widely understood industry tests, but not surprisingly do have some limitations in replicating full-scale testing (Blades, L., Douglas, R., McCullough, G. and Woods, A. (2014). Correlation of static aging effects on automotive catalysts. *Canadian J. Chemical Engineering* 92, 9, 1526-30); however they are widely used and understood tests in industry and appropriate to the pre-washcoat stage of catalyst development. In-situ aging tests for the initially tested catalysts are performed at 800 ºC under an air gas flow of 50 $ml \cdot min^{-1}$ for over 2 weeks (around 350 hrs), see Table S4 for details. The aged samples are then re-run through light-off experiments at same reaction conditions. Post-characterizations of the aged samples are carried out by SEM analysis and particle tracking. S

Simulated car exhaust conditions.

To evaluate the catalysts in realistic environments, CO+NO, diesel oxidation and ammonia slip reactions are tested. CO+NO model reaction was designed to evaluate the materials for the three-way catalytic converters. The tests were carried out in a temperature-programmed fixed-bed reactor by ramping up the temperature from 90 °C to 500 °C at a rate of 10 °C/min and using 0.2 g of catalyst mixed with 0.2 g of cordierite. The inlet concentrations were fixed to the concentrations of 4000 ppm CO and 4000 ppm NO, respectively, at a total flow of 12 L/min at N_2 balance. DOC (Diesel oxidation catalyst) model reaction was used to evaluate the use of the materials for real automotive catalytic converters. The tests were carried out in a steady state temperature-programmed reactor at the temperature range of 150 °C to 330 °C with a 10 min hold at each temperature stages. The total flow was 12 L/min at N_2 balance with the gas composition of 1450 ppm CO, 105 ppm propylene (C_3H_6), 125 ppm NO, and 4.5% CO_2, 10% O_2 and 5% H_2O (steam). Ammonia slip model reaction is to evaluate the possibility on removing excess NH_3 from the non-catalyzed NH_3. A steady state temperature-programmed reactions was carried out from 150 °C up to 330 °C with a 10 min hold at each temperature stages. Inlet conditions were 550 ppm NH_3, CO 220 ppm with 4.5% CO_2, 10% O_2 and 5% H_2O (steam) at the N_2 balanced total flow of 12 L/min. For the gas products analysis on each reaction, both inlet and outlet gases were measured by MKS MG2000 multi-gas analyser using a FT-IR detector. The conversions are calculated by the change of each gas concentrations and the light-off curves were plotted from the conversion values at each temperature stages. For a summary of catalytic testing conditions see S3.

Estimation of Turnover Frequency order of magnitude

To determine TOF, it is essential to have accurate catalytic surface areas; however the nature of the embedded interface makes this difficult to determine precisely. Characterization techniques such as CO temperature programmed desorption or CO-ITK (isotope transient kinetics) are possible to characterize the Pt particles, however these techniques yielded a broad response which did not give sufficiently accurate analysis at low Pt loading. This broad response may reflect contributions from different sites on the Pt and perovskite surfaces and their interface. We have therefore utilized a geometrically based model, estimating the surface area of the surface particles and calculating the surface area of emergent Pt hemispheres. This results in an estimated TOF value for lab-scale CO oxidation of 0.487 s^{-1}, whilst this is only an estimated value to give order of magnitude, it compares well with literature values [S-Y. Wang, N. Li, R-

Mei. Zhou, L.-Y. Jin, G-S. Hu, J-Q. Lu, M-F. Luo, *J. Mol. Catal., A: Chem.* 374–375 (2013) 53–58. The details of this analysis and comparisons are included in the supplementary information:

$$CO\ converison\ (\%) = \frac{[CO]_{In\ Vol\ \%} - [CO]_{out\ Vol\ \%}}{[CO]_{In\ Vol\ \%}}\ x\ 100$$

$$TOF_{180\,℃} = \frac{Conv_a\ x\ F_{CO}}{S_a}$$

TOF 180 ℃ is the Time of flight for 180 ℃ of Pt+LCT, $Conv_a$ is the conversion in % at 180 ℃, S_a is the number of active sites, F_{co} is the total flux rate of CO

$Conv_a$ =0.58 @180 ℃

S_a = 3.215 x 10^{-5}

F_{co} = 200ml^{-min}, so 3.33 x 10 x 10^{-5} moles/s^{-1}

Thus, (0.58 * 3.33 x 10^{-5}) / 3.215 x 10^{-5}

Therefore, TOF = 0.486 s^{-1}

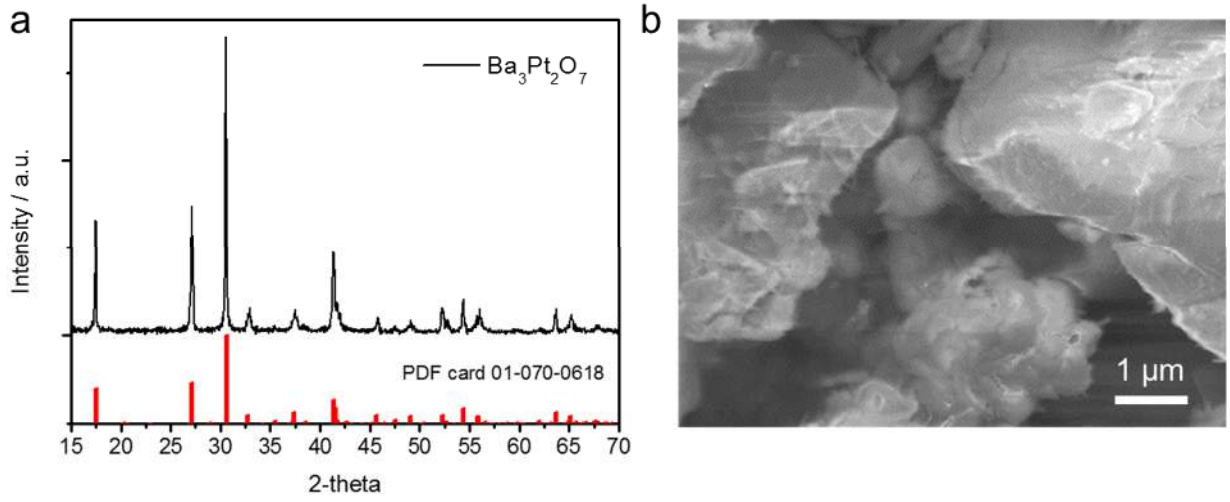

Fig. S1. $Ba_3Pt_2O_7$ characterization. (a) X-ray diffraction pattern in the case of laboratory made $Ba_3Pt_2O_7$ which well matched with the PDF card of 01-070-0618 and Inorganic Structural Database (ICSD) and (b) SEM image of the $Ba_3Pt_2O_7$ co-precursor.

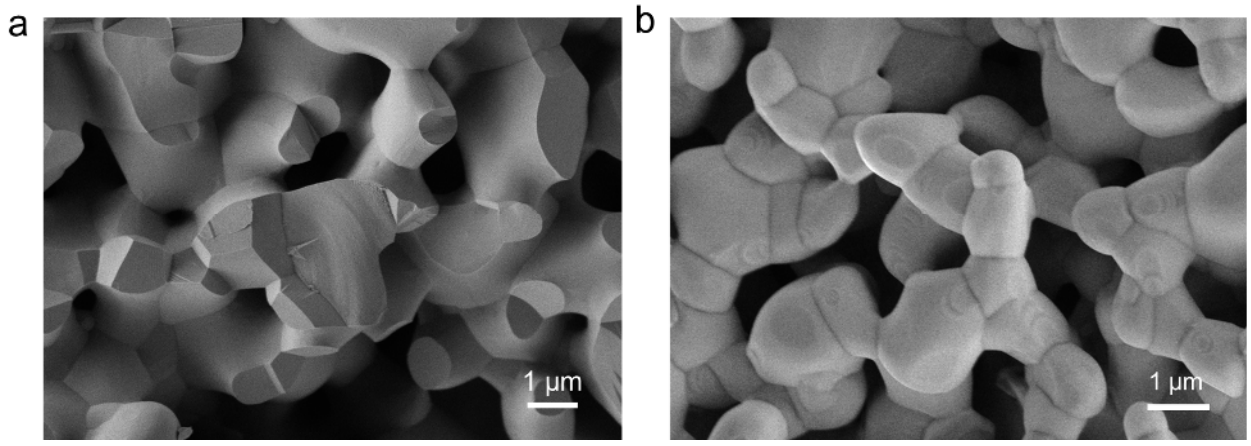

Fig. S2. Surface and microstructure analysis of as-prepared perovskites. SEM images for the (a) **LCT** ($La_{0.4}Ca_{0.4}TiO_3$) and (b) **LST** ($La_{0.4}Ca_{0.4}TiO_3$) perovskites.

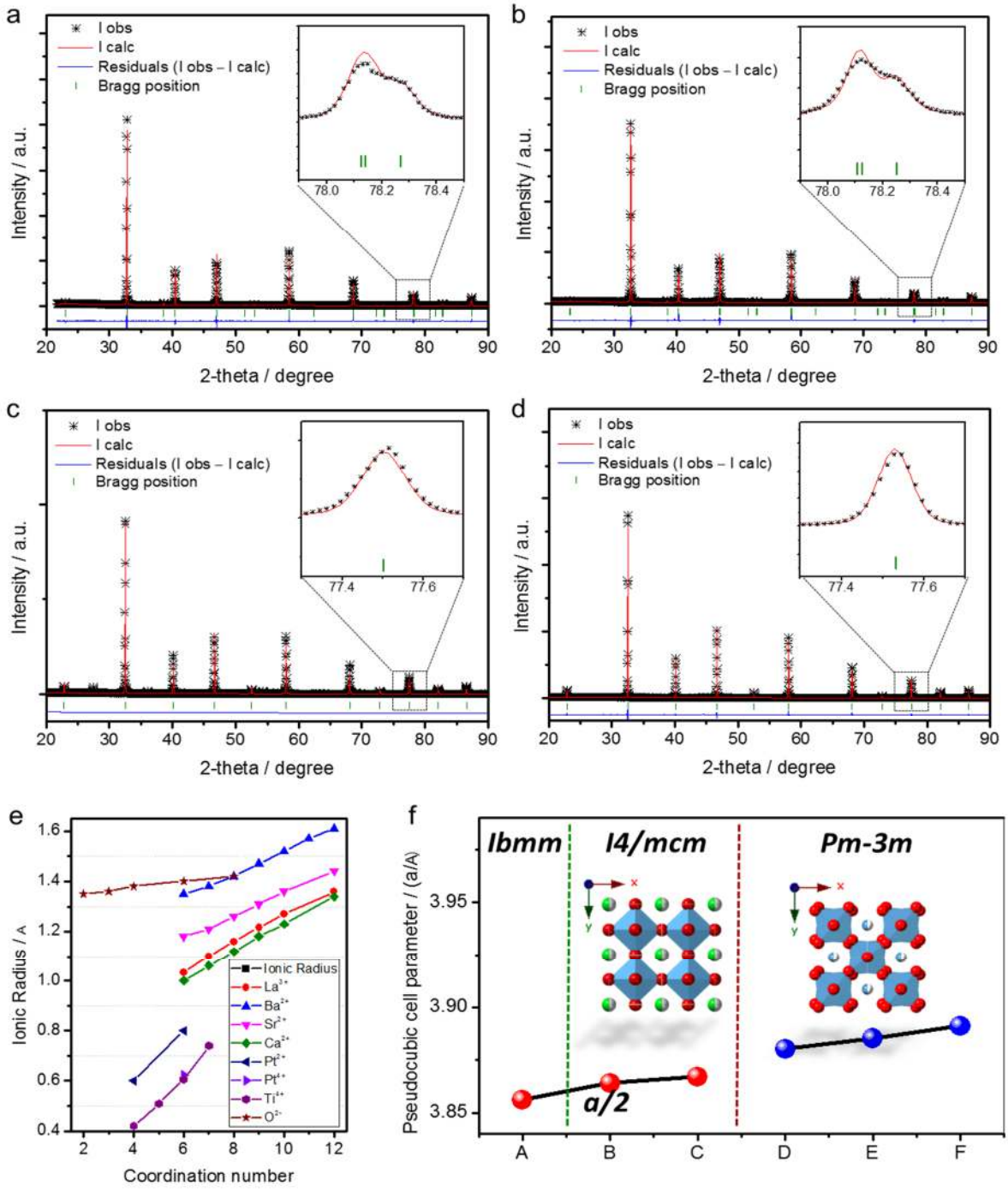

Fig. S3. Structural analysis of the Pt incorporated perovskites. Refined X-ray diffraction patterns using Rietveld analysis for (a) **LCT**, (b) **Pt@LCT**, (c) **LST** and (d) **Pt@LST** to investigate the structural difference. (e) Ionic radius versus coordination numbers for all used elements and (f) change of the cell parameters and XRD analysis for the prepared perovskites of A. $La_{0.4}Ca_{0.4}TiO_3$, B. $La_{0.4}Ca_{0.3925}Ba_{0.0075}TiO_3$, C. $La_{0.4}Ca_{0.3925}Ba_{0.0075}Pt_{0.005}Ti_{0.995}O_3$, D.

$La_{0.4}Sr_{0.4}TiO_3$, E. $La_{0.4}Sr_{0.3925}Ba_{0.0075}TiO_3$, and F. $La_{0.4}Sr_{0.3925}Ba_{0.0075}Pt_{0.005}Ti_{0.995}O_3$ with crystal structure images for both tetragonal **Pt@LCT** and cubic **Pt@LST** from (b) and (d).

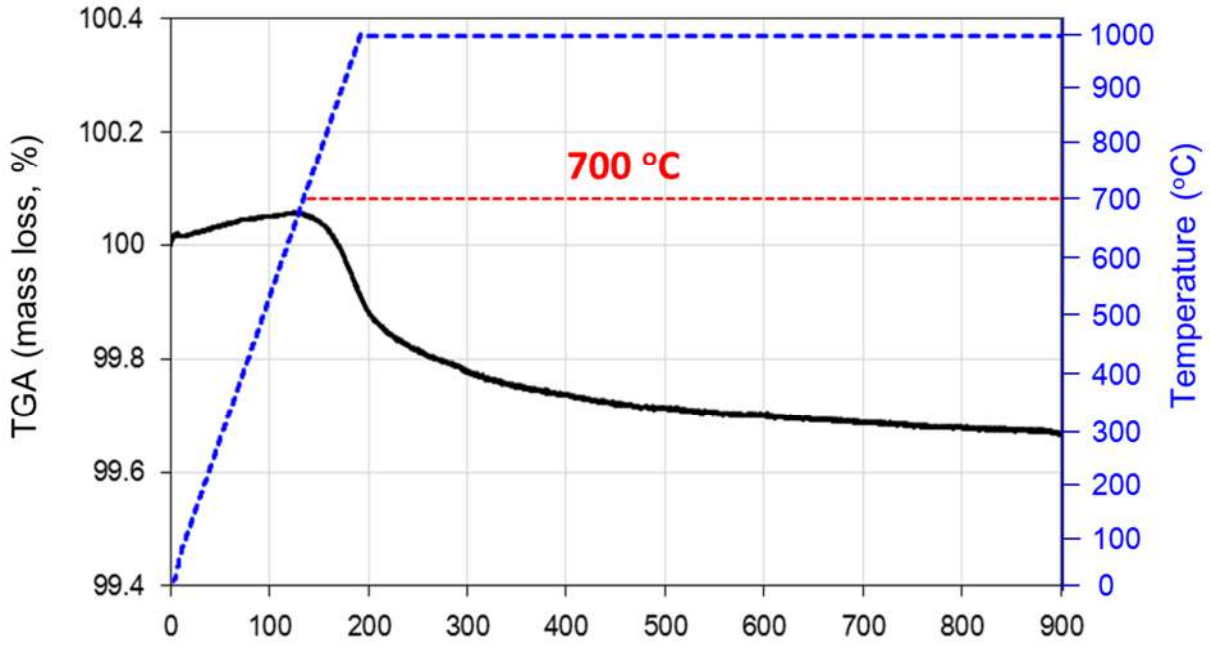

Fig. S4. Emergence behavior to optimise reduction conditions. TGA analysis of **Pt@LCT**, under measurement conditions: heat up to 1000 °C with a ramp rate of 5 °C min^{-1} hold for 12 hrs, in the gas atmosphere of 5% H_2/95% Ar (20ml/min).

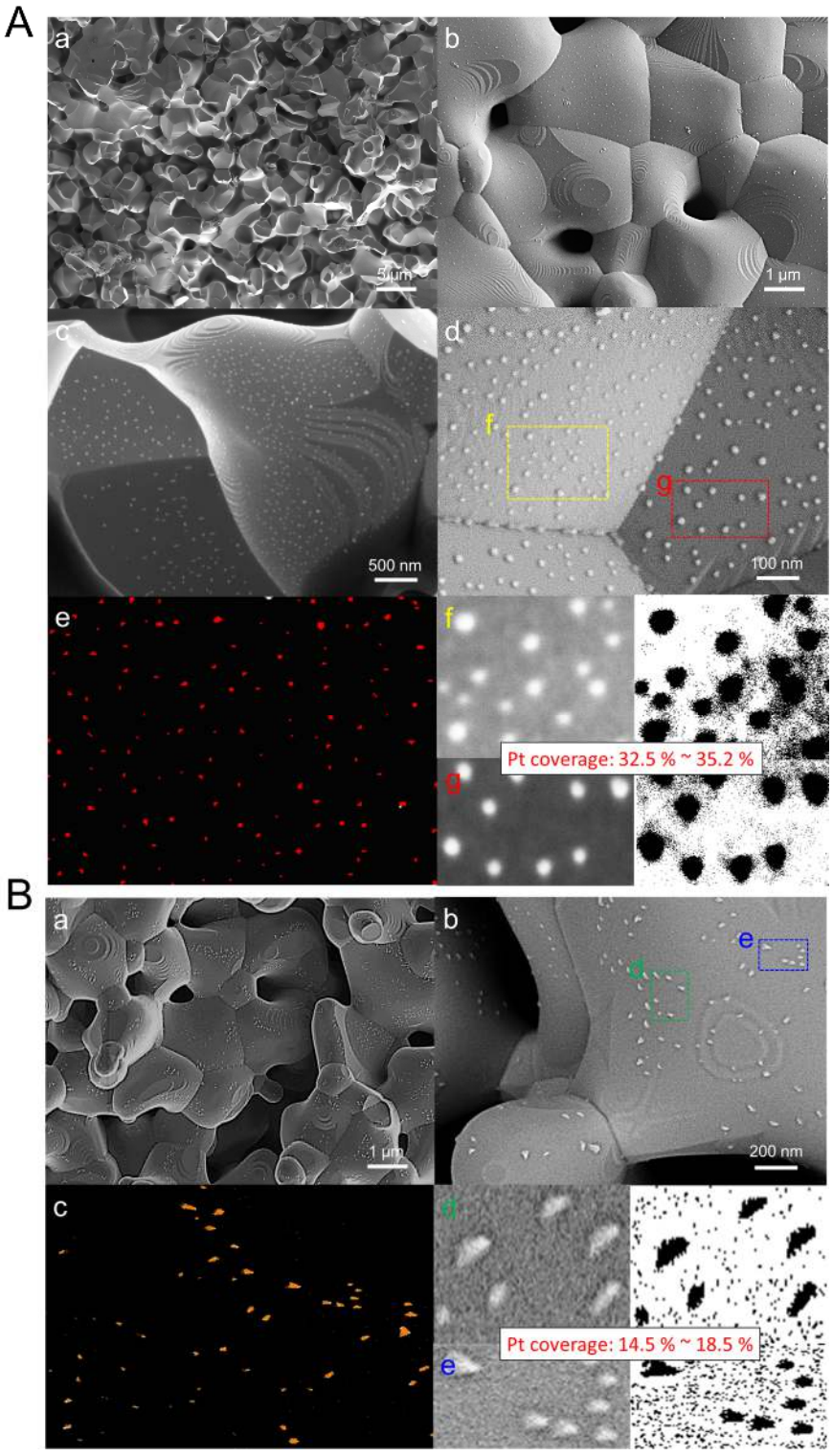

Fig. S5. Tracking of the emerged Pt NPs on the perovskite surfaces. SEM images for A. Pt+**LCT** and B. **Pt+LST** perovskites with various magnifications of A(a-d) and B(a-b), as well

as converted images to calculate the Pt particle size distributions and coverages at certain areas of A(e-g) and B(c-e), respectively.

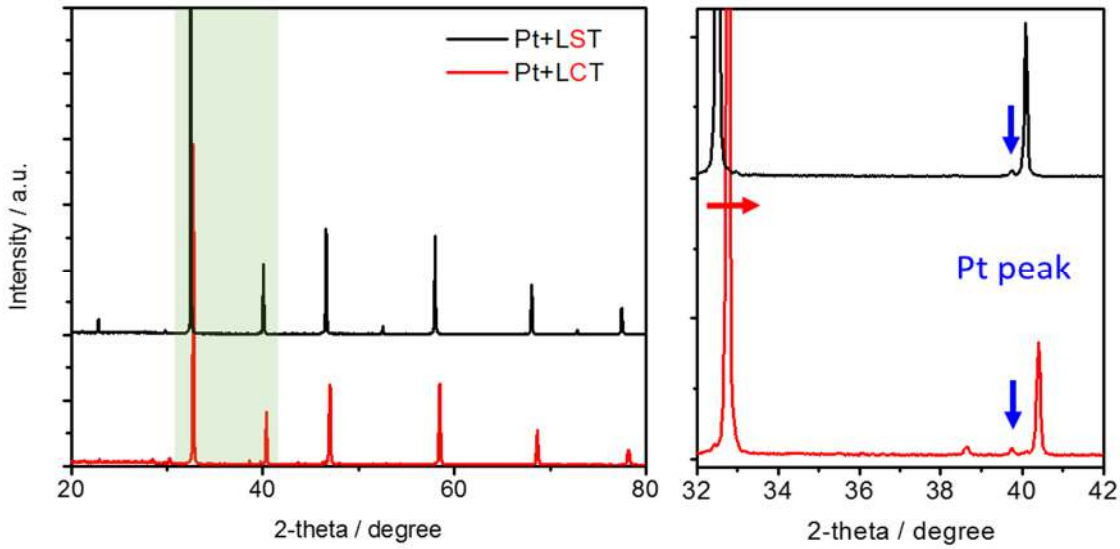

Fig. S6. XRD patterns (inset: magnification for 32°-42°) for the perovskites after Pt emergence. showing the well-defined, sharp reflections for face-centered cubic (fcc) Pt (38°-39.8°) (*3*). The perovskite peak shifts are due to the difference in cation size between Ca and Sr.

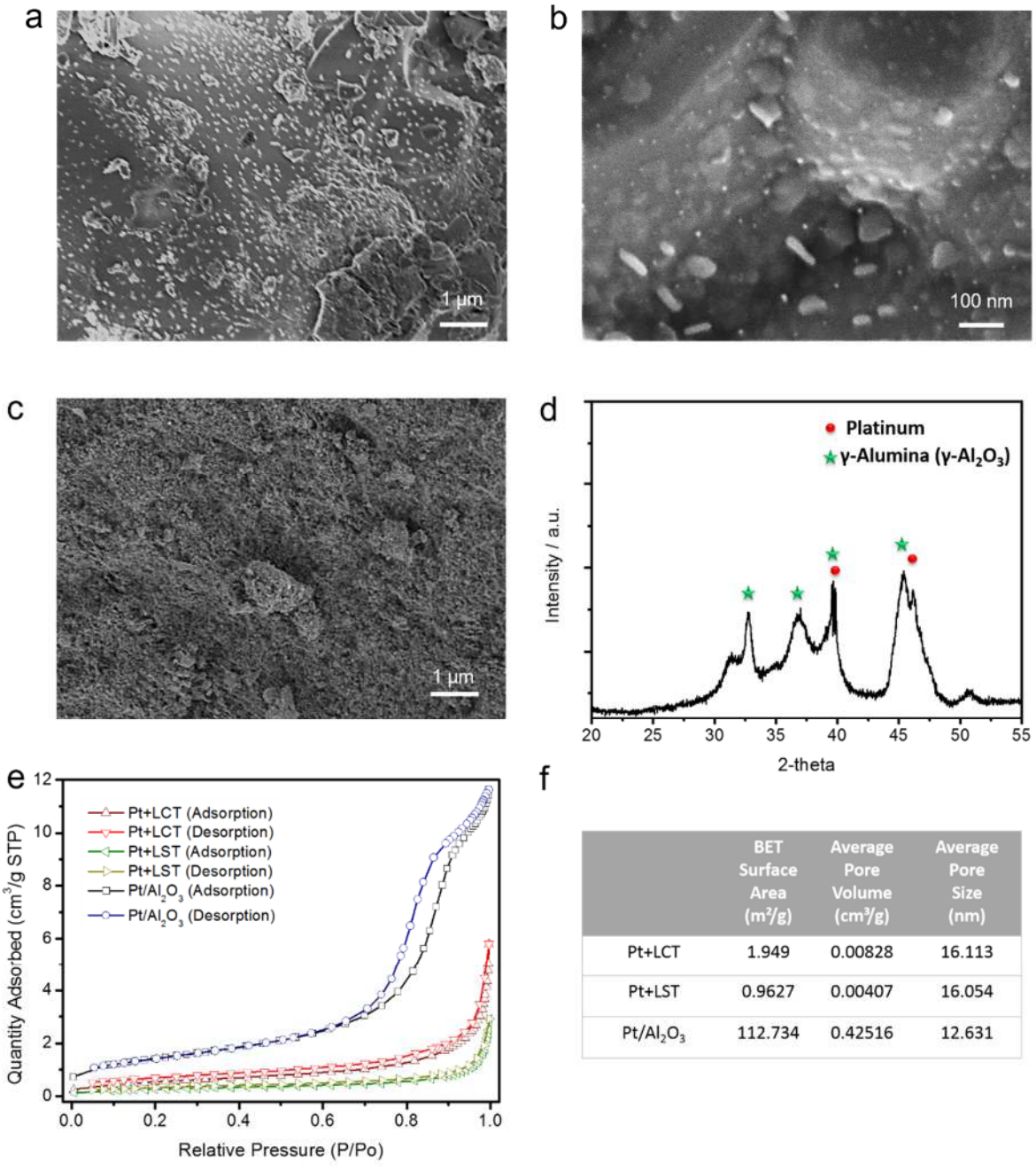

	BET Surface Area (m^2/g)	Average Pore Volume (cm^3/g)	Average Pore Size (nm)
Pt+LCT	1.949	0.00828	16.113
Pt+LST	0.9627	0.00407	16.054
Pt/Al_2O_3	112.734	0.42516	12.631

Fig. S7. Reference Pt impregnated catalysts. (a-b) SEM images for the **Pt/LCT**. (c) SEM image and (d) X-ray diffraction pattern for **Pt/γ-Al_2O_3**, as well as the (e) N_2-

adsorption/desorption analysis with (f) the summarized Table of **Pt+LCT** and (b) **Pt+LST** perovskites comparing with the **Pt/γ-Al_2O_3** catalyst..

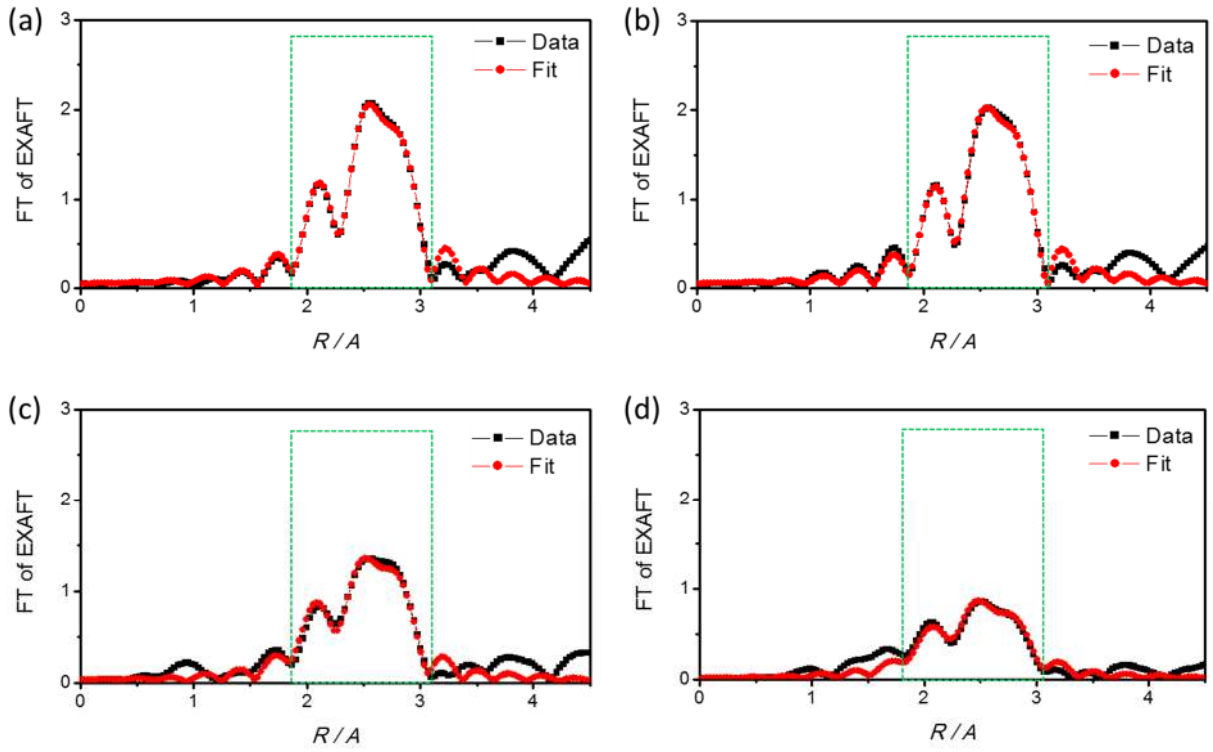

Fig. S8. Extended X-ray absorption fine structure. EXAFS data analysis of the Pt L_{III}-edge by comparing experimental data and the fitting curves (R-range=1.8-3.12 Å) for (a) Pt foil, (b) **Pt/γ-Al_2O_3**, (c) **Pt/LCT** and (d) **Pt+LCT.**

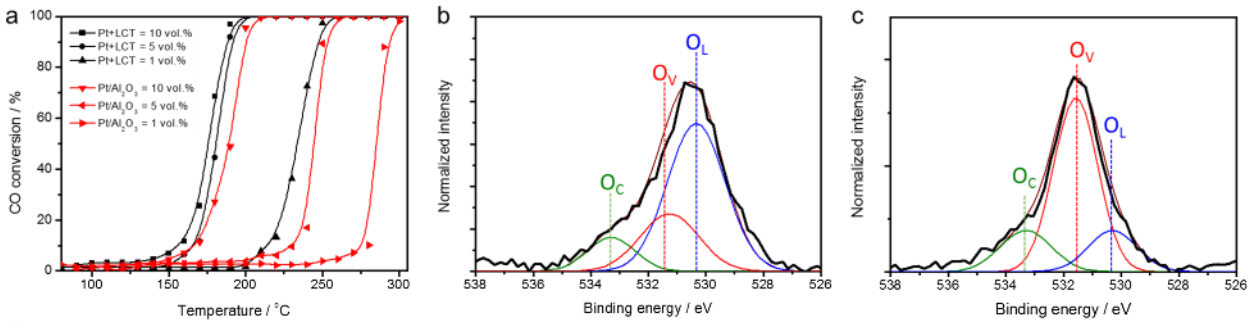

d

		Binding Energy (eV) and relative percentages in parentheses (%)			
		$O_L(O^{2-})$	$O_D(O^-)$	$O_C(O^-)$	$(O_D+O_C)/O_L$
Pt@LCT	eV	530.329	531.262	533.289	0.58
	%	63.36	28.89	11.75	
Pt+LCT	eV	530.306	531.58	533.305	4.86
	%	17.08	64.96	17.96	

Fig. S9. Oxygen partial pressure effect. (a) Light-off curves for CO oxidation at various oxygen partial pressures by a feed mixture gas of 20,000 ppm CO, 10.0 vol.% O_2 from air (21% O_2 and 79% N_2) at N_2 balance with a total gas flow rate of 200 ml/min (GHSV=60,000/hr) on the samples of **Pt@LCT** and **Pt/γ-Al$_2$O$_3$**. The reactivity of **Pt/γ-Al$_2$O$_3$** largely decreases at lower O_2 content, which is a normal phenomenon. XPS O 1s spectra of (b) **Pt@LCT** and (c) **Pt+LCT** after emergence process at 700 ºC with the heating and cooling rates of 5 °C·min^{-1} under continuous flow of 5% H_2/Ar (20 ml·min^{-1}). (d) summarized table for binding energies (eV) and relative percentages for each oxygen species on the surface and the calculated $(O_D+O_C)/O_L$ ratio for **Pt@LCT** before and after the emergence process. (O_L: lattice oxygen, O_D: defects or surface oxygen, and O_C: chemisorbed oxygen species on the surface) (*4, 21*).

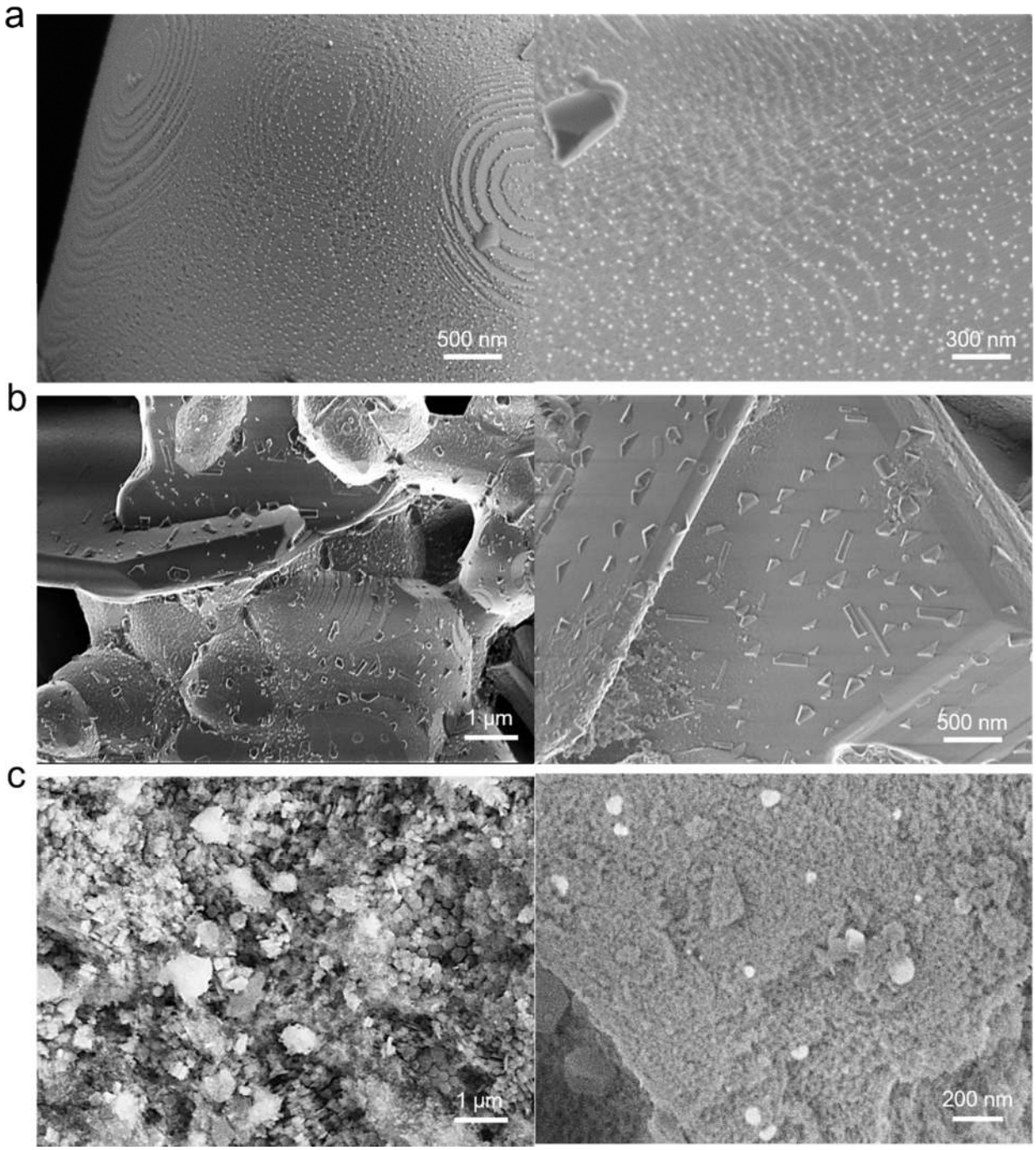

Fig. S10. Pt NPs analysis after long-term aging test. SEM images of (a) **Pt+LCT**, (b) **Pt/LCT** and (c) **Pt/γ-Al_2O_3**, after aging tests at 800 ºC under an air gas flow of 50 ml/min for over 2 weeks (350 hrs).

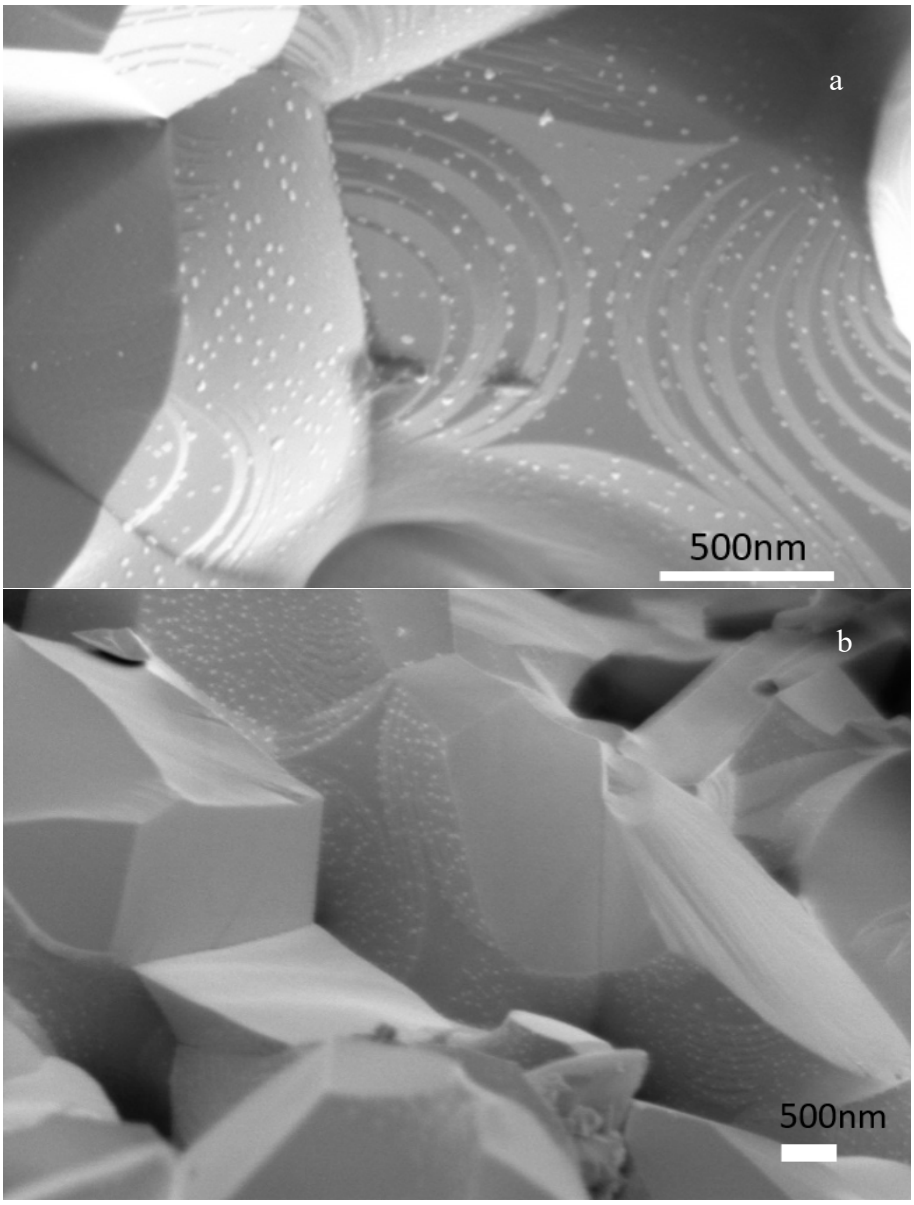

Figure S11a shows a portion of a crushed Pt+LCT pellet that has been reduced in 5%H_2/Ar at 700°C for 12 hours, then thermally aged under air 95%/steam 5% in at 800°C for 12 hours at the University of St Andrews, see table S4 aging 1 for details~~.~~.

Figure S11b shows a Pt+LCT pellet that has been reduced in 5%H_2/Ar at 700°C for 12 hours, then thermally aged in Johnson Matthey's ~~static~~ ager for 12 hours with 10% H_2O at 800°C, see table S4 aging 2.. Here, the pellet has been cleaved after reduction and ageing, showing emergence toward exposed surfaces during reduction, whilst the cleaved surfaces have no nanoparticles.

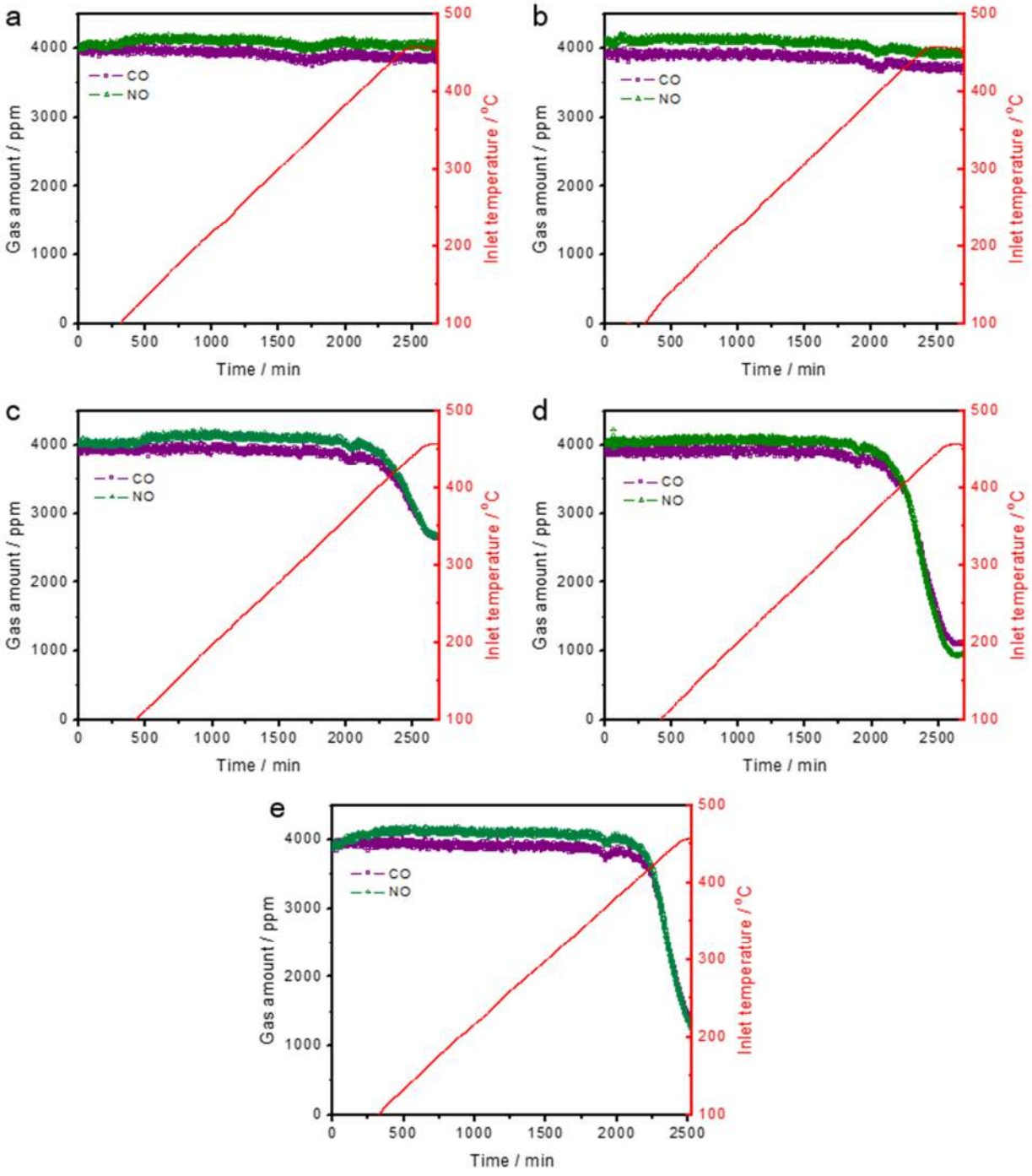

Fig. S12. Catalyst tests of CO+NO reaction in simulated car exhaust environments. Each reactant amounts (ppm) for (a) **LCT**, (b) **Pt@LCT**, (c) **Pt/LCT**, (d) **Pt+LCT** and (e) **Pt/γ-Al_2O_3** over the time and reaction temperature.

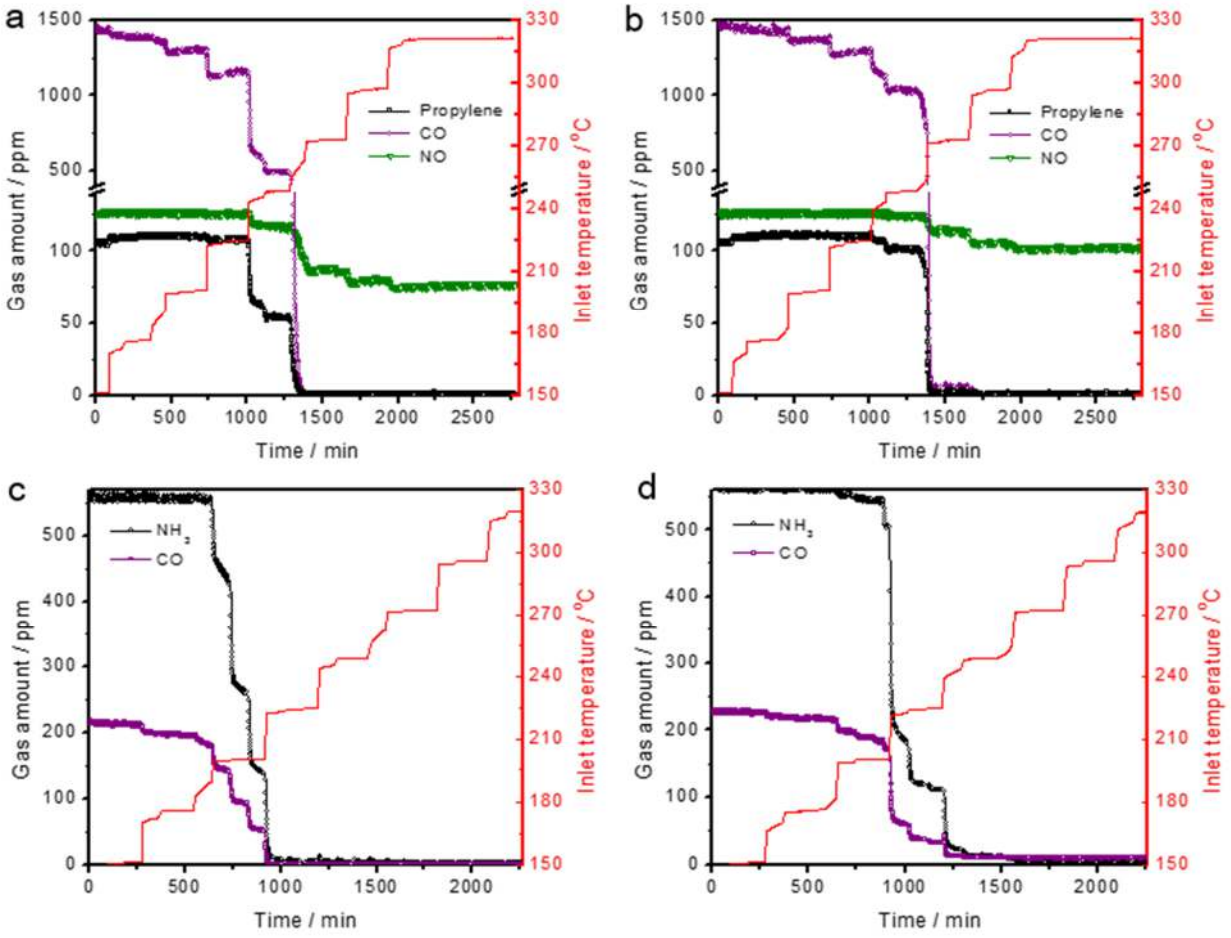

Fig. S13. DOC oxidation in real car exhaust environments and simulated ammonia slip tests. Each reactant amounts (ppm) of the DOC and AMOX tests for (a and c) **Pt+LCT** and (b and d) **Pt/γ-Al_2O_3**, respectively, over the reaction time and temperature.

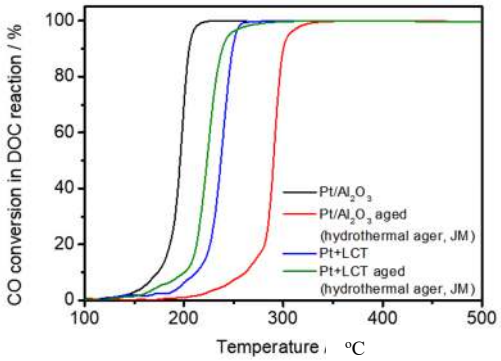

Figure S14 shows the results on fresh and aged samples, which have been aged in the Hydrothermal ager and tested DOC conditions S4 (Aging-3) (please refer to Table S3 for the summary of the operating conditions). shows light off in DOC conditions (2) before and after ageing in a hydrothermal ager

Table S1. The estimated crystallographic parameters from the powder x-ray diffraction data of literature and all the prepared perovskites taken at room temperature.

	$La_{0.4}Ca_{0.4}TiO_3$	$La_{0.4}Ca_{0.3925}Ba_{0.0075}TiO_3$	$La_{0.4}Ca_{0.3925}Ba_{0.0075}Pt_{0.005}Ti_{0.995}O_3$	$La_{0.4}Sr_{0.4}TiO_3$	$La_{0.4}Sr_{0.3925}Ba_{0.0075}TiO_3$	$La_{0.4}Sr_{0.3925}Ba_{0.0075}Pt_{0.005}Ti_{0.995}O_3$
	Ibmm[22]	*I4/mcm*	*I4/mcm*	*Pm-3m*	*Pm-3m*	*Pm-3m*
			Cell Parameter			
a/Å	7.7120	7.7287	7.7329	3.8802	3.8852	3.8911
b/Å	7.7278	7.7287	7.7329	3.8802	3.8852	3.8911
c/Å	7.7278	7.8120	7.8090	3.8802	3.8852	3.8911
β/°	90	90	90	90	90	90
Volume/Å^3	460.55	461.66	462.41	58.42	58.64	58.91

Table S2. Structural parameters by EXAFS fitting of (a) Pt foil, (b) **Pt/γ-Al_2O_3**, (c) **Pt/LCT** and (d) **Pt+LCT** for the Pt-Pt atomic layer based on the coordination number of 12.

Samples	S_0^2	σ^2	*R* (Å)	delr	ΔE0 (eV)	R-factor
(a)	0.836 (+/- 0.029)	0.00474 (+/- 0.00017)	2.76347	-0.01063 (+/- 0.0015)	8.352 (+/- 0.3)	0.0013624
(b)	0.754 (+/- 0.037)	0.00429 (+/- 0.00024)	2.76187	-0.01223 (+/- 0.0021)	7.660 (+/- 0.4)	0.0025838
(c)	0.708 (+/- 0.057)	0.00580 (+/- 0.00044)	2.75510	-0.01900 (+/- 0.0039)	4.918 (+/- 0.7)	0.0083257
(d)	0.530 (+/- 0.049)	0.00685 (+/- 0.00057)	2.73417	-0.03993 (+/- 0.0051)	6.564 (+/- 0.9)	0.0106468

Table S3. Reaction conditions

	Lab-scale CO oxidation (St Andrews University)	**NH_3 oxidation** (Johnson Matthey)	**CO+NO 1:1 reaction** (Johnson Matthey)	**Diesel oxidation (1)** (Johnson Matthey)	**Diesel oxidation (2)** (Johnson Matthey)
Gas Mix	CO 20000ppm, O_2 10.0 vol.% (from air 21% O_2 and 79% N_2) -Carrier: N_2 balance	NH_3 550ppm, CO 220ppm, 4.5% CO_2, 10% O_2, 5% H_2O (steam) -Carrier: N_2 balance	CO 4000ppm, NO 4000ppm - Carrier: N_2 balance	C_3H_6 200ppm, NO 300ppm, CO 1500ppm, 4.5% CO_2, 10% O_2, 5% H_2O (steam) - Carrier: N_2 balance	20000ppm in total: CO 1550ppm, NO 160 ppm, CH_4 40ppm, C_3H_6 40ppm (propylene), C_7H_8 20ppm (Toluene), $C_{10}H_{22}$ 30ppm (Decane), 5% CO_2 5% H_2O (steam), - Carrier: N_2 balance

Flow Rate and GHSV	Flow through catalyst bed: 200 ml·min^{-1} GHSV: 60,000/hr (in grain catalyst), 11,000/hr (assuming 3g/in^3 coating)	Flow through catalyst bed: 2L/min GHSV: 110,000/h (assuming 3g/in^3 coating)	Flow through catalyst bed: 2L/min GHSV: 110,000/h (assuming 3g/in^3 coating)	Flow through catalyst bed: 2L/min GHSV: 110,000/h (assuming 3g/in^3 coating)	Flow through catalyst bed: 2L/min GHSV: 110,000/h (assuming 3g/in^3 coating)
Catalyst amount, diluent and size	200 mg (220-380 µm)	0.2g with 0.2g of cordierite (250-355 µm)	0.2g with 0.2g of cordierite (250-355 µm)	0.2g with 0.2g of cordierite (250-355 µm)	0.2g with 0.2g of cordierite (250-355 µm)
Temperature range	70-300 ºC	150-330 °C	90-500 °C	150-330 °C	100-500 °C
Ageing furnace used	Static furnace (St Andrews)	Static furnace (JM) with 10% steam	Redox ager (JM) with 10% steam	Static ager (JM) with 10% steam	Static ager (JM) with 10% steam
Analyser used	Gas Chromatography	MKS MG2000 multi-gas analyser using a FT-IR detector	MKS MG2000 multi-gas analyser using a FT-IR detector	MKS MG2000 multi-gas analyser using a FT-IR detector	MKS MG2000 multi-gas analyser using a FT-IR

Table S4. Ageing conditions

Aging-1	Static ager (University of St Andrews)
H_2O	5%
AIR	95%
Ramp rate	10 °C/min
Max. Temp.	800 °C

Aging-2	Static ager (Johnson Matthey)
H_2O	10 %
AIR	90 %
Ramp rate	10 °C/min
Max. Temp.	800 °C

Aging-3	TWC hydrothermal redox ager (Johnson Matthey)	
	Base mix	+ perturbation line
Time	5 min	5 min
NO	0.1 %	
H_2O	10 %	
CO	0.5 %	
O_2	0.27 %	0.80 %
N_2	Balance	
Ramp rate	10 °C/min	
Max. Temp.	950 °C	